

Dipole Antenna with Horn Waveguide for Energy Harvesting in DTV Systems

Watcharaphon Naktong¹ and Natchayathorn Wattikornsirikul^{2, *}

Abstract—This article presents a dipole antenna using an I-shape adding technique on both sides of the antenna's body to widen the frequency range, using a horn waveguide to gain enhancement and harvest energy by matching the circuit which is compatible with the voltage multiplier circuit at the RF frequency (510–790 MHz) in a TV digital system. Having measured the effect of the antenna, it was found that the antenna operates at a frequency range of 60.24% (450–838 MHz), a 67.79% increase from the base dipole antenna, which has again enhancement of 10.23 dB from adding the horn waveguide (60.99%). It has a pattern of energy radiating in a specific direction, and when the antenna is used with an energy harvesting circuit to get energy or power from the front direction of the TV digital antenna at a distance of 10 km, it is capable of harvesting energy of up to 7.33 μ W.

1. INTRODUCTION

The energy required to charge small mobile or wireless devices is an essential factor in human life. To help people work faster, in terms of living a comfortable life, for today's use of human power, it is widely used and consumes a lot of energy. If it still consumes conventional energy, that would have a serious impact on the economic and social development of many countries [1]. Due to this problem, many researchers have developed new forms of renewable energy, such as solar energy [2], biomass energy [3], wind energy [4], thermal energy [5], and radio frequency energy (RF), such as the digital TV, mobile, and WiFi frequency range [6–15]. Due to the foregoing, researchers have been interested in developing the field of energy harvesting from radio frequency (RF) that uses a receiver antenna and AC to DC power conversion circuit. This research shows an I-shaped stub dipole antenna at the top side for use in the range of 521–557 MHz in the DTV system. This is connected with a low pass filter rectifier L type and cockcroft-walton, to help to increase the efficiency of energy harvesting. The transmission towers will use the Tokyo facility with a power level of 69 kW, tested at a distance of approximately 25 km from the transmission towers, which is capable of converting power to 0.2 V. It is about 43.1% effective [16]. The array-jointed rectangular microstrip antenna is used to harvest wave energy in the frequency range of 470–2400 MHz in DTV, LTE700 GSM900, GSM1800, and WiFi systems. By designing a rectifier using a high frequency diode BAT17, the power can be converted to 0.2 V [17]. The Log-periodic antenna is arranged in a circular polarization pattern. It is used to harvest wave energy in DTV (450–900 MHz), LTE700, and GSM900 frequencies. By using a novel hybrid resistance compression technique (HRCT) to increase the efficiency of energy harvesting, the transmission towers are selected in Liverpool with -10 dBm power, which can increase the power conversion by approximately 66.7 μ W and has an overall conversion efficiency of 42.2% [18]. A nested ring antenna is used to cover the 1710–2690 MHz frequency range in GSM1800 and WiFi as a means of improving energy harvesting efficiency. The power

Received 1 April 2022, Accepted 7 June 2022, Scheduled 5 July 2022

* Corresponding author: Natchayathorn Wattikornsirikul (natchayathorn.w@rmutp.ac.th).

¹ Department of Telecommunications Engineering, Faculty of Engineering and Technology, Rajamangala University of Technology Isan, Nakhon Ratchasima 30000, Thailand. ² Department of Electronics and Telecommunications Engineering, Faculty of Engineering, Rajamangala University of Technology Phra Nakhon, Bangkok 10300, Thailand.

conversion can be increased by approximately $6\ \mu\text{W}$, with an overall conversion efficiency of 57% [19]. An array-jointed rectangular microstrip antenna is used to harvest wave energy in the frequency range of 470–2400 MHz in DTV, LTE700 GSM900, GSM1800, and WiFi systems. By designing a rectifier using HSMS286c high-frequency diode, the energy conversion efficiency is 65% [20]. An oval dipole antenna surrounded by a rectangular ring is used to increase the efficiency of the gain, with a rectangular reflector equal to 6.6 dBi. It is designed for use in the GSM900 system. By using a height or high frequency diode HSMS 2850 to convert AC to DC power, at a testing distance of approximately 1 meter from the transmission tower, it is capable of transmitting power at $27.6\ \mu\text{W}$ and also, of converting power to $5.3\ \mu\text{W}$ [21]. Later, oval dipole antenna was further developed by adding a rectangular reflector from the research [21,22], resulting in a higher gain of 9.2 dBi [23]. An The discone antenna had a circular disc to cover the use of DCS 1800 and UMTS 2100 systems. By designing the rectifier, the Dickson 2-Stage Rectifier uses a high-frequency diode HSMS 2850, tested at a distance of approximately 200 meters from the transmission towers, which is capable of converting $0.02\ \text{W}/\text{m}^2$ of power [24].

The mesh dipole antenna was created by inkjet printing with hybrid material. When the structure was made thinner and the impedance increased for use with the rectifier circuit by the log-periodic transmission antenna to transmit the power of 3 W at a power testing distance of approximately 1.1 m with a frequency of 920 MHz, it can convert the energy to $0.65\ \mu\text{W}/\text{m}^2$ with an efficiency of approximately 55%. A frequency of 940 MHz can convert the power to $0.9\ \mu\text{W}/\text{m}^2$, with an efficiency of approximately 64.80% [25]. The discone antenna with a circle plate covers a frequency range of 650–5000 MHz in the DTV, LTE700, GSM900, GSM1800, and WiFi systems. When designing the rectifier circuit, the Dickson 2-Stage Rectifier used a high-frequency diode HSMS 2850. By testing the distance at frequency of 900 MHz, the distance from the transmission tower was approximately 0.7 m, which can be converted into a power of 0.3 V, with an efficiency about 13%. At a frequency of 2,450 MHz, the distance from the transmission tower (about 0.35 m) can convert the energy to 0.303 V, with an efficiency of approximately 16% [26]. The double bow-tie dipole antenna with a front and back side used in the frequency range UHF-TV, connected to the rectifier circuit, can convert energy up to $231\ \mu\text{W}$, and the frequency range of 91.1 MHz in the FM system can convert energy up to $885\ \mu\text{W}$ [27].

According to the research mentioned, it has the advantage of increasing the efficiency of the gain in energy harvesting, but there are also disadvantages in terms of gain optimization and much complexity with more adjusting points. As a result, the researchers choose disadvantages identified by this research that is the first part of a basic dipole antenna structure [27, 28] with an increasing I-shaped stub to widen the frequency [16, 29–32] and gain enhancement for the antenna by using the horn waveguide [33–35] and in terms of getting more energy. The second part studies the matching impedance circuit using a Radial Stub Circuit (RSC) [20, 36, 37] with the power frequency signal converter circuit by using a full-wave rectifier circuit with a voltage multiplier circuit [16, 38, 39] to increase the pressure on the rectenna system that is designed to receive power at a frequency of 510–790 MHz, which is the digital TV wireless transmission system. At present, it is widely used in Thailand [40].

The design calculation and simulation of the antenna structure are compared with the measurement results for the determination of the antenna properties, presented in Section 2. In Section 3 the energy harvesting system is presented. Section 4 compares the results of the antenna with an energy harvesting circuit with the previous research, and the final conclusions will be presented in Section 5.

2. ANTENNA STRUCTURE DESIGN AND ANTENNA PROPERTIES MEASUREMENT

2.1. Antenna Structure Design

Antenna structure design uses a dipole, an antenna structure to add a quadrilateral stub to both sides of the antenna body [28–32], as shown in Figure 1. It is designed at a mid-range frequency of 650 MHz of the 510–790 MHz frequency range, which has a bandwidth impedance of $75\ \Omega$, on a copper plate with a thickness of the base material of $h = 0.02\ \text{cm}$ and conductivity of the conductor material $\sigma = 5.8 \times 10^7\ \text{S}/\text{m}$. The antenna width parameters are calculated as shown in Equation (1). The width of the antenna ($W = 23.21\ \text{cm}$) is calculated as given in (1) [28]:

$$W = \frac{0.5c}{f_r} \quad (1)$$

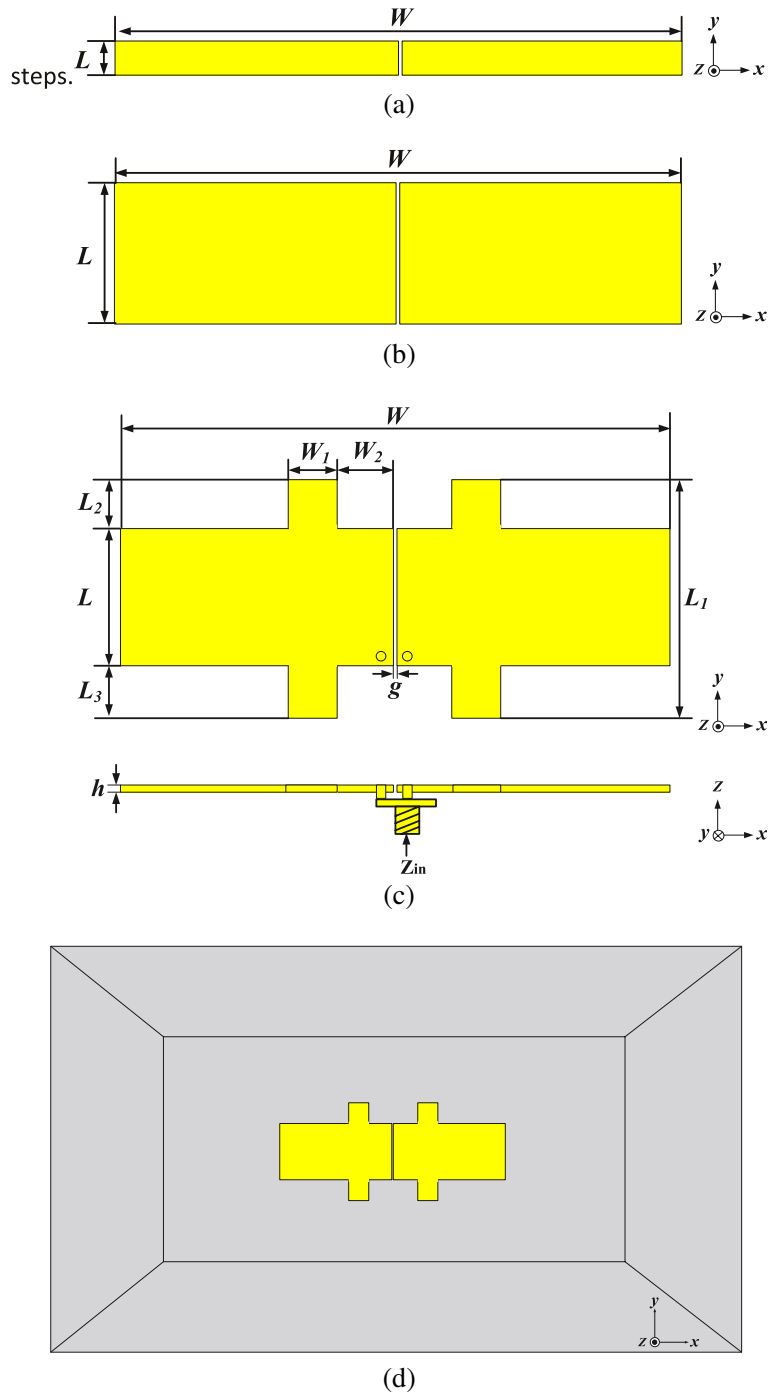


Figure 1. Antenna configuration turning steps, (a) step 1, (b) step 2, (c) step 3, (d) step 4.

Calculating the length of the antenna ($L = 2.88 \text{ cm}$) is given in (2)

$$L = \frac{0.015c}{f_r} \tag{2}$$

Calculating the width of the gap between EBG and the antenna ($g = 0.1 \text{ cm}$) is given in (3)

$$g = \frac{0.002c}{f_r} \tag{3}$$

The part of structure turning is shown in Figures 1(a)–(d). The calculation of the gap width in Figure 1(c) is as shown in Equation (3). By the adjustment, the principle can be divided into 3 main parts. We obtained the results for the characteristic impedance derived from a design by the experimental method with the reflection coefficient electrical simulation program $|S_{11}|$ (dB) by completing the following steps.

We chose to simulate the results on the CST simulator. Turning has a 3 part antenna structure that is more effective if the first part adjusts the length L of the dipole antenna structure [28] as shown in Figure 1(b). By studying the current density compared to the wavelength of the antenna, it was found that the region from the input point to the middle of the antenna had the current density that affected the wavelength change the most. The simulation results at low frequency 510 MHz are shown in Figure 2, with constant width $W = 23.12$ cm, and adjusting only for the lengths from the wavelength 3.8 cm, 4.8 cm, 5.8 cm, 6.8 cm, and 7.8 cm [30]. It was found that the appropriate parameter was $L = 5.8$ cm. From the adjustment, it was found that it had a frequency of use range of 19.40% (563–684 MHz), whose width was increased from 56 MHz to 121 MHz or 116.07% but still did not cover the frequency range of 510–790 MHz as there was need as shown in Figure 2 to continue adjusting in the second part.

In the second part, the technique of increasing the frequency of use range was achieved by adding an I-shaped stub to both sides [29–32]. By designing in the range of 790 MHz high frequency ($W_1 = 0.026\lambda$) and length ($L_1 = 0.25\lambda$), as shown in Figure 1(c), study with simulated current density at high frequency

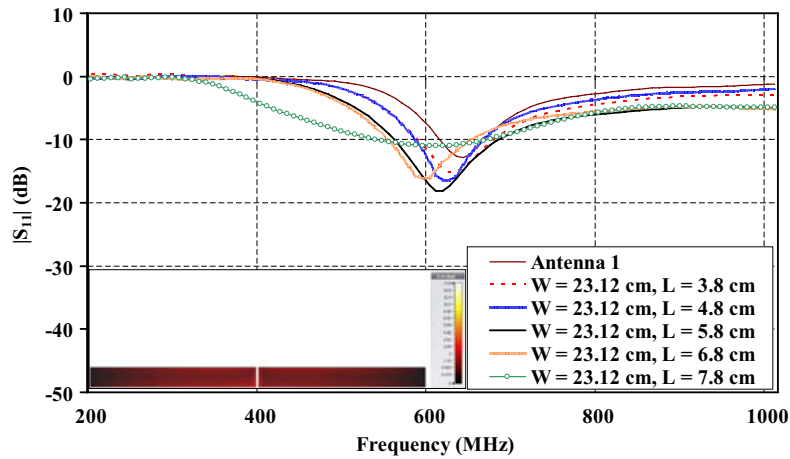


Figure 2. Simulated result $|S_{11}|$ (dB) value when adjusted for W and L .

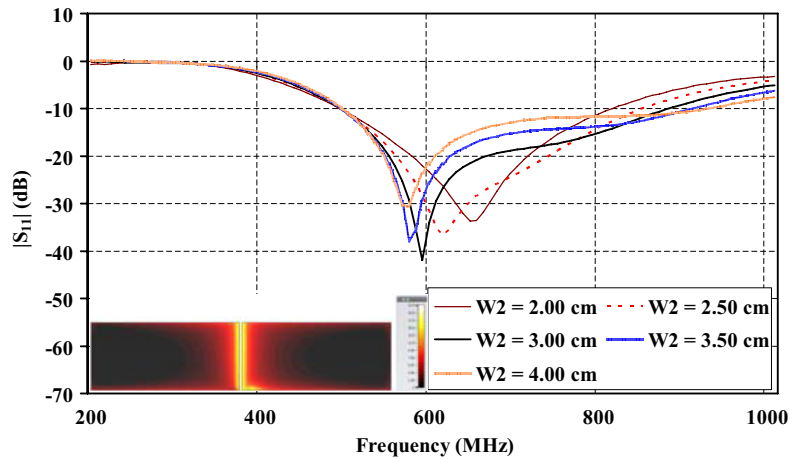


Figure 3. Simulated result $|S_{11}|$ (dB) value when adjusted W_2 .

of 790 MHz is shown in Figure 3. The width parameter values W_2 beginning to be adjusted from $(0.052\lambda < W_2 < 0.105\lambda)$ were 2 cm, 2.5 cm, 3 cm, 3.5 cm, and 4 cm. It was found that the appropriate parameter was $W_2 = 3$ cm, at a parameter of the length constant $L_2 = L_3 = 1.85$ cm. It is found in the adjustment that it has a frequency of use range of 56.87% (458–822 MHz), which covers the frequency range of 510–790 MHz as required, as shown in Figure 3 with a width increase from 56 MHz to 364 MHz or 116.07%.

In this part of the study, we focus on the expansion gain by horn waveguide structure [33–35], as shown in Figure 1(d). A reflector is built on a galvanized sheet with a thickness of 0.02 cm, designed at a 650 MHz mid-frequency. The adjustment is determined by distance H according to the wavelength value at frequency 650 MHz, which affects the best bandwidth impedance value by starting to adjust from $(0.260\lambda < H < 0.433\lambda)$ that were 12 cm, 14 cm, 16 cm, 18 cm, and 20 cm, and it was found that the appropriate parameter was $H = 16$ cm. From a notice in the part of 54.60% (458–802 MHz) using a frequency range with, as shown in Figure 4, the highest expansion rate of 10.26 dBi, the result was better than the distances of 18 cm and 20 cm, with expansion rates of 9.95 dBi and 9.81 dBi, as shown in Figure 5 respectively at 500–800 MHz, which affects the antenna box size. As it is actually built, it affects the budget and installation space, when adding the dipole antenna structure together with the horn waveguide, as shown in Figure 6. This was adjusted in order to obtain the best parameters, as shown as in Table 1.

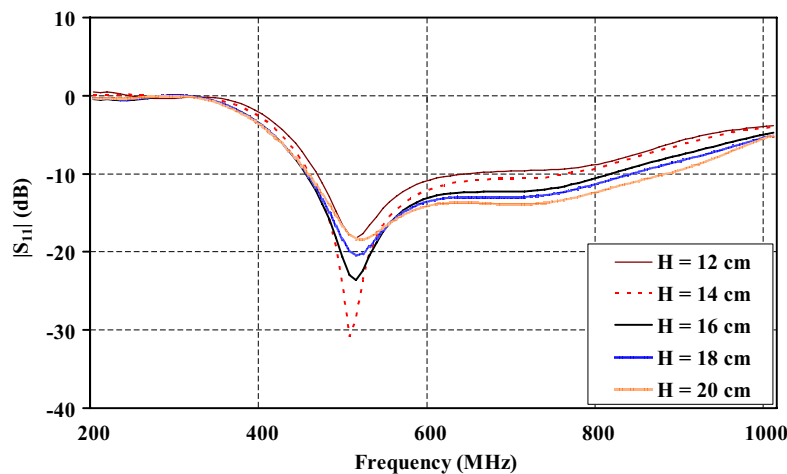


Figure 4. Simulated result $|S_{11}|$ (dB) value when the H was adjusted.

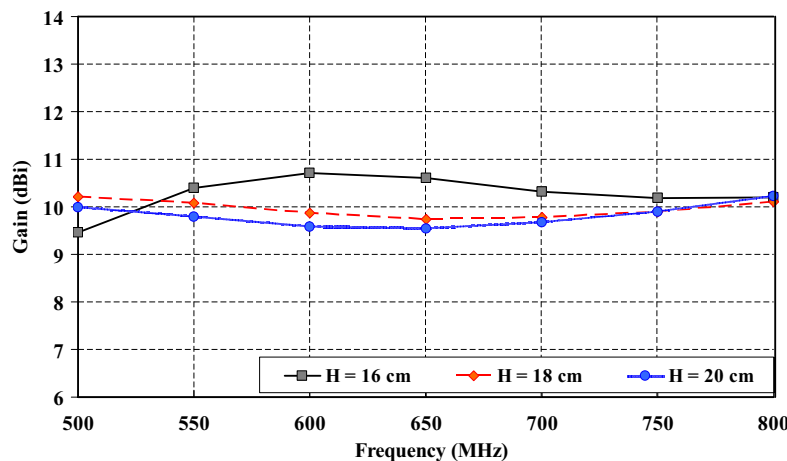


Figure 5. Simulated result of the expansion rate when H was adjusted.

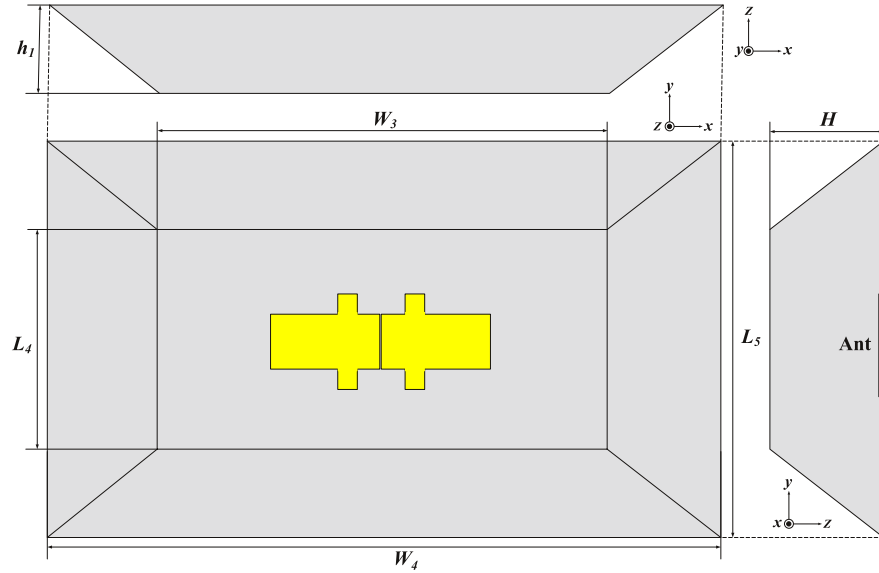


Figure 6. Designed dipole antenna.

Table 1. Values of various variable sizes.

Dimensions	Size (cm)
Width of the dipole antenna (W)	23.1
Width of the I-shaped stub (W_1)	1.85
Width of the I-shaped stub to feed line (W_2)	3
Width of the base Horn Waveguide (W_3)	46
Width of the horn waveguide (W_4)	69
Length of the dipole antenna (L)	5.8
Length of the I-shaped stub (L_1)	9.5
Length of the I-shaped stub up (L_2)	1.85
Length of the I-shaped stub up (L_3)	1.85
Length of the base Horn Waveguide (L_4)	23.1
Length of the Horn Waveguide (L_5)	44
Hight of the Horn Waveguide to dipole antenna (H)	16
Thick of the dipole antenna (h)	0.02
Hight of the Horn Waveguide (h_1)	16
The gap of the dipole antenna and ground plane (g)	0.1

2.2. Measurement of the Antenna Properties

When the appropriate parameters of the antenna were obtained according to Table 1, a prototype dipole antenna was constructed, as shown in Figure 7(a), with a horn waveguide, as shown in Figure 7(b). Then it was measured with a Network Analyzer model E5071 which found that the bandwidth impedance value of the prototype dipole antenna had a 61.37% (454–856 MHz) frequency range. Moreover, the dipole antenna with a horn waveguide has a 60.24% (450–838 MHz) frequency range, as shown in Figure 8. In comparison, it was found that the trend was in the same direction. This includes the gain value measured at the frequency of 500–800 MHz, as shown in Figure 9, which can be clearly displayed in numbers, as in Table 2.



Figure 7. Test instrument and the prototype dipole antenna with horn waveguide. (a) Dipole antenna. (b) A prototype dipole antenna with horn waveguide.

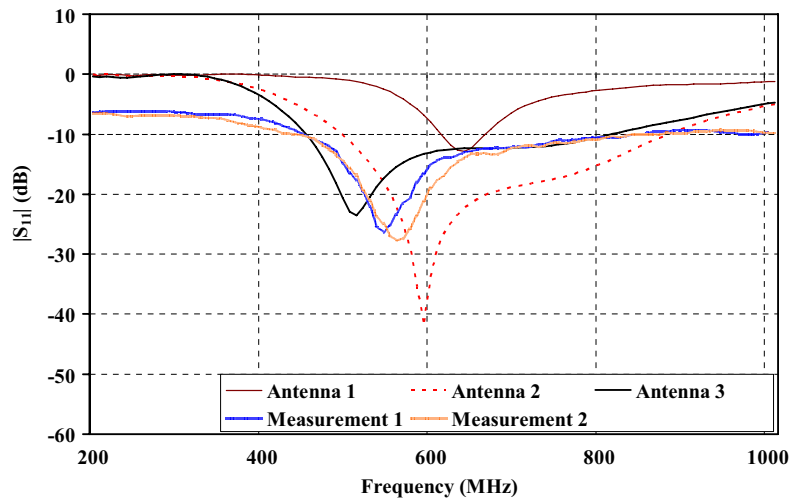


Figure 8. The result of the comparison of the simulated values with the actual measurements of the values $|S_{11}|$ (dB).

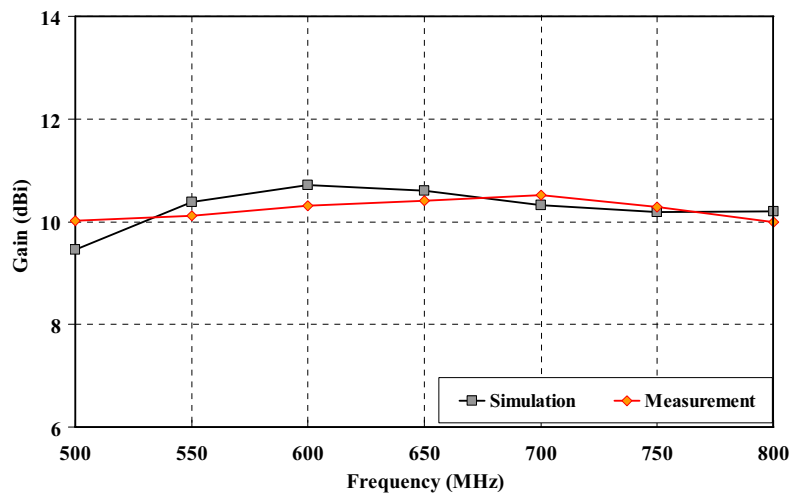


Figure 9. The result of the comparison of the simulated values with the actual measurement of gain.

Table 2. Comparison of impedance bandwidth and gain.

comparison		$ S_{11} $ (dB)	Gain (dBi)
Simulated	Dipole antenna	19.40% (563–684 MHz)	1.88
	Dipole antenna prototype	56.87% (458–822 MHz)	4.15
	Dipole antenna prototype with horn waveguide	54.60% (458–802 MHz)	10.26
Measured	Dipole antenna prototype	61.37% (454–856 MHz)	3.99
	Dipole antenna prototype with horn waveguide	60.24% (450–838 MHz)	10.23

A comparison of the energy radiated results was selected at a 3 frequency range. The most logical approach is to use the low-frequency range 510 MHz, frequency 650 MHz, and high frequency 790 MHz in the plane of the electric field as shown in Figure 10 and in the plane of the magnetic field as shown in Figure 11. From the comparison of energy radiated results, it was found that the pattern of energy radiation was directional. That conforms with the structure of the horn waveguide in front of the antenna. There was a similar pattern of energy radiating in both planes: namely, the electric and magnetic fields, due to the advantages that the antenna structure is not complicated.

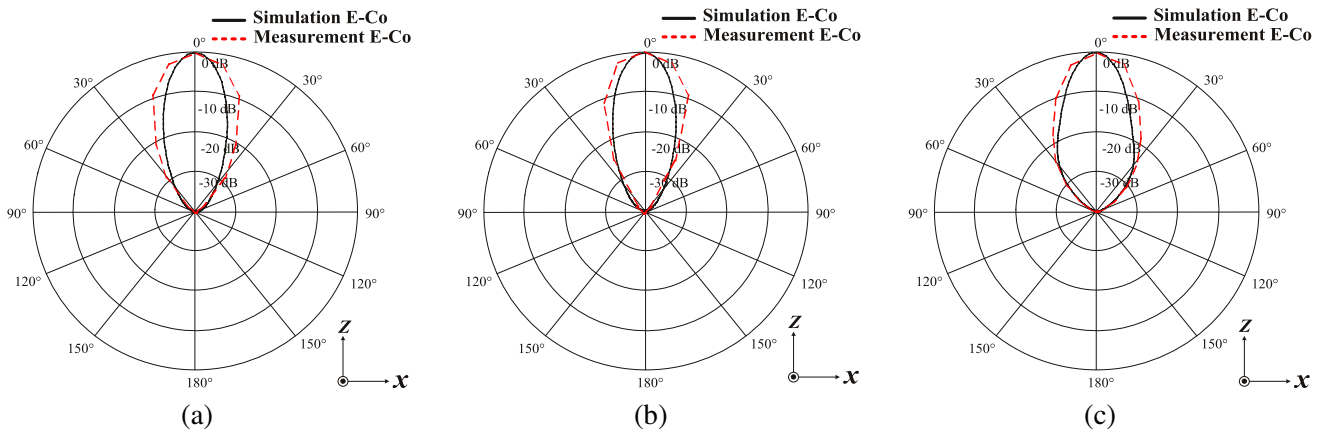


Figure 10. Comparison of simulation with measurement results of the electric field radiation energy form. (a) 510 MHz, (b) 650 MHz, (c) 790 MHz.

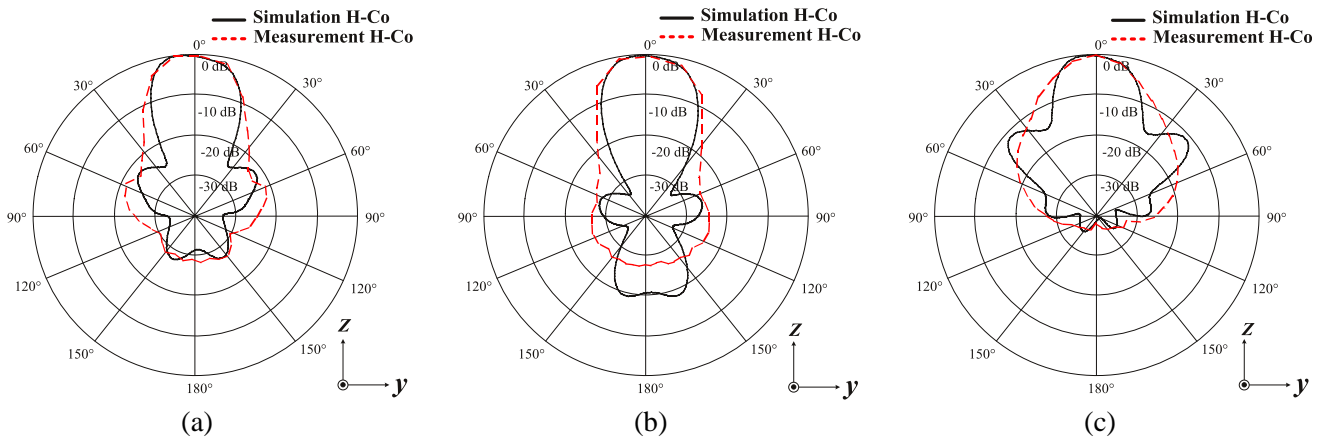


Figure 11. Comparison of simulation with measurement results of the magnetic field radiation energy form. (a) 510 MHz, (b) 650 MHz, (c) 790 MHz.

3. RECTENNA

The matching impedance circuit uses a Radial Stub Circuit (RSC) [36, 37], as shown in Figure 12, to maximize the signal source’s energy transfer by design at a center frequency of 650 MHz which has a half power beamwidth $R = 3\text{ cm}$, $\theta = 60^\circ$. The input impedance of the electric load, then the half-power beam was adjusted to a width of $R = 3\text{ cm}$ with a value of $\theta = 60^\circ$, then it started to be adjusted from ($60^\circ < \theta < 166^\circ$), namely 60° , 103° , and 166° , and it was found that the optimum half-power beam was $R = 2.6\text{ cm}$ and had $\theta = 103^\circ$. Adjusting showed that it has the using frequency range 510–790 MHz as desired, as shown in Figure 12, where the efficiency of the connection with a rectenna is higher than 50%. Within a frequency range from 2.2 to 2.6 GHz at 13 dBm, we obtained energy when $100\ \Omega$ was loaded, and the increased rectenna energy storage efficiency is 80.25%, as shown in Figure 13.

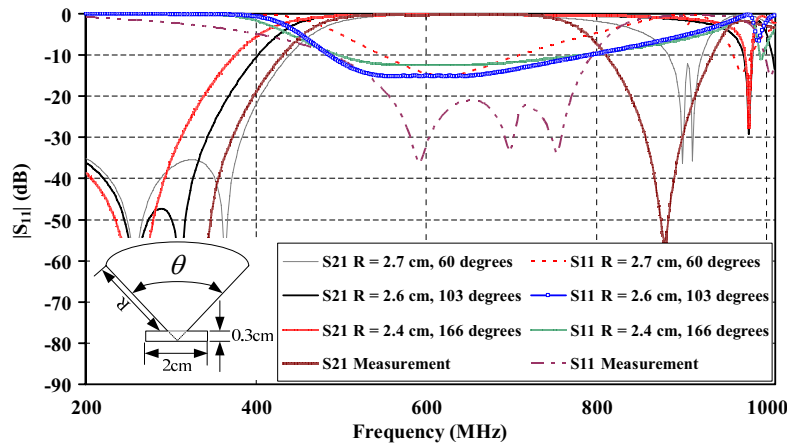


Figure 12. Simulation and measurement frequency responses of the proposed BPF.

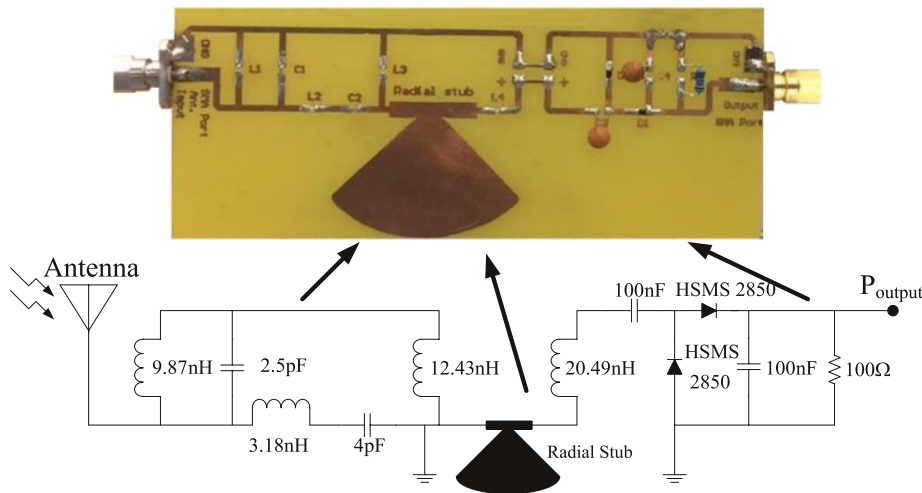


Figure 13. Matching impedance circuit 510–790 MHz [4].

In terms of the measurement of DC energy [38, 39] that was obtained by connecting the prototype antenna to the rectifier and voltage multiplier circuits as the block diagram show in Figure 14, this was tested on the 4, 6, 8, and 10 times voltage multiplier circuit, which had a voltage of 0.29 V, 0.31 V, 0.28 V, and 0.27 V, respectively. From the aforementioned, the 6 times voltage multiplier circuit has the highest voltage value of 0.31 V and a power value of 7.33 μW . In the test measurement, the voltage

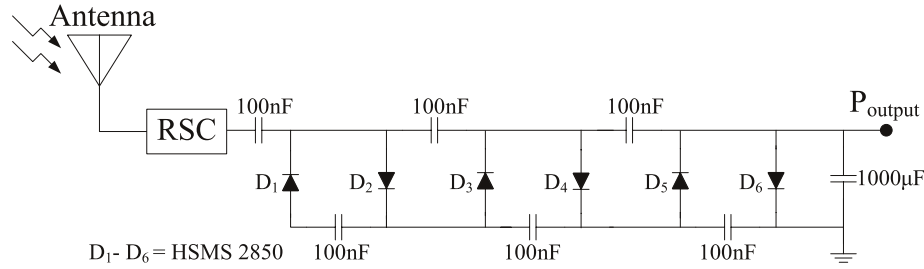


Figure 14. Matching circuit with 6 times voltage multiplier circuit.

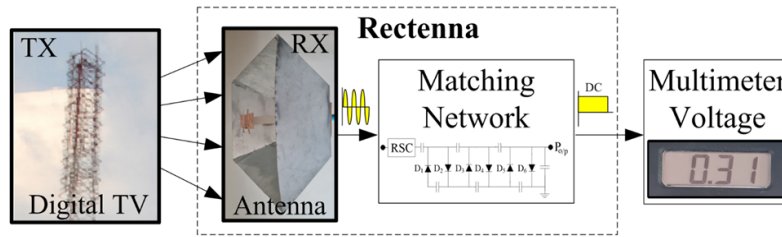


Figure 15. Block diagram of ambient RF energy harvesting.

value in a real aria has a temperature variable that is taken into account, and the value starts from 22° to 36°. The results were measured for 1 hour and recorded every 10 minutes to obtain the best average. From the test, it was found that at temperatures from 22° to 32°, the voltage was 0.31 V while at temperatures from 33° to 37°, the voltage was the highest 0.307–0.309 V, with a different value of 64%. By trying to measure energy in Muang District, Nakhon Ratchasima Province, Thailand, which has the most suitable receiving signals distance 10 km in the front direction of the transmission tower, we took measurement using the voltage and current module ADS1115 16-Bit ADC, microcontroller board Arduino Uno R3 display on LCD screen, as shown in Figure 15.

4. COMPARISON OF RESEARCH

The study and design of the dipole antenna structure with the energy harvesting circuit were compared with the research shown in Table 3. The antenna has the advantage of a simple, uncomplicated antenna structure. It has a high gain of 10.23 dB. That affects the efficiency more as well, which is equal to 63.57%. There is another advantage in terms of transmitting powerless –20 dBm, but it can receive power more efficiently than the research stated.

Table 3. Comparison efficiency of rectenna.

Reference	Frequency (GHz)	Substrate	Antenna size (cm ³)	Input Power (dBm)	Gain (dB)	Efficiency (%)
[7]	0.55–2.5	FR4	16 × 16 × 0.16	–5	3.5	67
[16]	0.5	FR4	24.35 × 1.215 × 0.28	–15	-	48.9
[18]	0.47–0.88	FR4	16 × 16 × 0.16	–35	3.5	42.2
[20]	0.6–3	Rogers	7 × 4.8 × 0.0813	17	6	65
[26]	0.65–5	FR4 copper	12 × 12 × 0.16 18 × 12 × 11	5	5.4	16
[27]	0.47–0.6	FR4	30.4 × 30.4 × 0.16	–20	-	28
Proposed	0.4–0.83	copper zinc	23 × 9.5 × 0.2 69 × 44 × 16	–20	10.23	63.57

5. CONCLUSION

To study the dipole antenna, we undertook fine adjusting, adding an I-shaped stub to widen the use frequency range and place it in front of the horn waveguide. To increase the gain and energy harvesting circuit, we used a multiplier circuit and made it more efficient. Using the measurement results to compare the simulation of the antenna properties, it was found that the use range was 60.24% (450–838 MHz) with an increase from the base dipole antenna of 19.40% (563–684 MHz), representing 67.79%, and the gain of the dipole antenna with a Waveguide Horn Prototype was enhanced from 3.99 dB to 10.23 dB, while the efficiency gain of 60.99% in the forward direction of the transmission tower was found to be 7.33 μ W with an efficiency value of 63.57%, which is another advantage. The antenna structure is simple and has few adjusting points.

ACKNOWLEDGMENT

Thanks to the Department of Electronic and Telecommunications Engineering, Faculty of Engineering, Rajamangala University of Technology Phra Nakhon and Department of Telecommunications Engineering, Faculty of Engineering and Technology, Rajamangala University of Technology Isan for supporting this research.

REFERENCES

1. Yang, Y., S. Bremner, C. Menictas, and M. Kay, "Battery energy storage system size determination in renewable energy systems: A review," *Renewable and Sustainable Energy Reviews*, Vol. 91, 109–125, 2018.
2. Oh, T. H., M. Hasanuzzaman, J. Selvaraj, S. C. Teo, and S. C. Chua, "Energy policy and alternative energy in Malaysia: Issues and challenges for sustainable growth — An update," *Renewable and Sustainable Energy Reviews*, Vol. 81, 3021–3031, 2018.
3. Sherwood, J., "The significance of biomass in a circular economy," *Bioresource Technology*, Vol. 300, 122755, 2020.
4. Karnauskas, K. B., J. K. Lundquist, and L. Zhang, "Southward shift of the global wind energy resource under high carbon dioxide emissions," *Nature Geoscience*, Vol. 11, No. 1, 38–43, 2018.
5. Kumar, K. R., N. K. Chaitanya, and N. S. Kumar, "Solar thermal energy technologies and its applications for process heating and power generation — A review," *Journal of Cleaner Production*, Vol. 282, 125296, 2021.
6. Kim, S., R. Vyas, J. Bito, K. Niotaki, A. Collado, A. Georgiadis, and M. M. Tentzeris, "Ambient RF energy-harvesting technologies for self-sustainable standalone wireless sensor platforms," *Proceedings of the IEEE*, Vol. 102, No. 11, 1649–1666, 2014.
7. Song, C., Y. Huang, P. Carter, J. Zhou, S. Yuan, Q. Xu, and M. Kod, "A novel six-band dual CP rectenna using improved impedance matching technique for ambient RF energy harvesting," *IEEE Transactions on Antennas and Propagation*, Vol. 64, No. 7, 3160–3171, 2016.
8. Saeed, W., N. Shoalb, H. M. Cheema, and M. U. Khan, "RF energy harvesting for ubiquitous, zero power wireless sensors," *International Journal of Antennas and Propagation*, Vol. 2018, 2018.
9. Shen, S., C. Y. Chiu, and R. D. Murch, "Multiport pixel rectenna for ambient RF energy harvesting," *IEEE Transactions on Antennas and Propagation*, Vol. 66, No. 2, 644–656, 2017.
10. Wagih, M., A. S. Weddell, and S. Beeby, "Rectennas for radio-frequency energy harvesting and wireless power transfer: A review of antenna design [antenna applications corner]," *IEEE Antennas and Propagation Magazine*, Vol. 62, No. 5, 95–107, 2020.
11. Chandrasekaran, K. T., K. Agarwal, A. Alphones, R. Mittra, and M. F. Karim, "Compact dual-band metamaterial-based high-efficiency rectenna: An application for ambient electromagnetic energy harvesting," *IEEE Antennas and Propagation Magazine*, Vol. 62, No. 3, 18–29, 2020.
12. Joseph, S. D., Y. Huang, and S. S. Hsu, "Transmission lines-based impedance matching technique for broadband rectifier," *IEEE Access*, Vol. 9, 4665–4672, 2020.

13. Gu, X., P. Burasa, S. Hemour, and K. Wu, "Recycling ambient RF energy: Far-field wireless power transfer and harmonic backscattering," *IEEE Microwave Magazine*, Vol. 22, No. 9, 60–78, 2021.
14. Erkmen, F. and O. M. Ramahi, "A scalable, dual-polarized absorber surface for electromagnetic energy harvesting and wireless power transfer," *IEEE Transactions on Microwave Theory and Techniques*, Vol. 69, No. 9, 4021–4028, 2021.
15. Bougas, I. D., M. S. Papadopoulou, A. D. Boursianis, K. Kokkinidis, and S. K. Goudos, "State-of-the-art techniques in RF energy harvesting circuits," *Telecom*, Vol. 2, No. 4, 369–389, Multidisciplinary Digital Publishing Institute, December 2021.
16. Furuta, T., M. Ito, N. Nambo, K. Itoh, K. Noguchi, and J. Ida, "The 500 MHz band low power rectenna for DTV in the Tokyo area," *2016 IEEE Wireless Power Transfer Conference (WPTC)*, 1–3, IEEE, May 2016.
17. Dhiman, L. and S. Singh, "Design and optimization of DGS based T-stub microstrip patch antenna for wireless applications," *Advancements in Engineering and Technology*, 631, 2015.
18. Song, C., Y. Huang, J. Zhou, and P. Carter, "Improved ultrawideband rectennas using hybrid resistance compression technique," *IEEE Transactions on Antennas and Propagation*, Vol. 65, No. 4, 2057–2062, 2017.
19. Palazzi, V., J. Hester, J. Bitto, F. Alimenti, C. Kallalakis, A. Collado, and M. M. Tentzeris, "A novel ultra-lightweight multiband rectenna on paper for RF energy harvesting in the next generation LTE bands," *IEEE Transactions on Microwave Theory and Techniques*, Vol. 66, No. 1, 366–379, 2017.
20. Zheng, S., W. Liu, and Y. Pan, "Design of an ultra-wideband high-efficiency rectifier for wireless power transmission and harvesting applications," *IEEE Transactions on Industrial Informatics*, Vol. 15, No. 6, 3334–3342, 2018.
21. Loubet, G., A. Takacs, and D. Dragomirescu, "Implementation of a battery-free wireless sensor for cyber-physical systems dedicated to structural health monitoring applications," *IEEE Access*, Vol. 7, 24679–24690, 2019.
22. Okba, A., A. Takacs, and H. Aubert, "Compact rectennas for ultra-low-power wireless transmission applications," *IEEE Transactions on Microwave Theory and Techniques*, Vol. 67, No. 5, 1697–1707, 2019.
23. Loubet, G., A. Takacs, E. Gardner, A. De Luca, F. Udrea, and D. Dragomirescu, "LoRaWAN battery-free wireless sensors network designed for structural health monitoring in the construction domain," *Sensors*, Vol. 19, No. 7, 1510, 2019.
24. Tampouratzis, M. G., D. Vouyioukas, D. Stratakis, and T. Yioultsis, "Use ultra-wideband discone rectenna for broadband RF energy harvesting applications," *Technologies*, Vol. 8, No. 2, 21, 2020.
25. Wagih, M., A. S. Weddell, and S. Beeby, "Meshed high-impedance matching network-free rectenna optimized for additive manufacturing," *IEEE Open Journal of Antennas and Propagation*, Vol. 1, 615–626, 2020.
26. Chuma, E. L., Y. Iano, and L. L. B. Roger, "Ultra-wide band rectenna design with discone antenna and rectifier with high impedance inductor," *2021 5th International Symposium on Instrumentation Systems, Circuits and Transducers (INSCIT)*, 1–6, IEEE, August 2021.
27. Jung, E. M., W. S. Lee, R. J. Vyas, and M. M. Tentzeris, "A wideband, quasi-isotropic, ambient RF energy harvester combining UHF-TV and FM," *IEEE Antennas and Wireless Propagation Letters*, Vol. 20, No. 10, 1854–1858, 2021.
28. Balanis, C. A., *Antenna Theory: Analysis and Design*, John Wiley & Sons, 2015.
29. Wang, C. J. and Y. L. Lee, "A compact dipole antenna for DTV applications by utilizing L-shaped stub and coupling strip," *IEEE Transactions on Antennas and Propagation*, Vol. 62, No. 12, 6515–6519, 2014.
30. Komsing, S., N. Fhaffhiem, A. Innok, and A. Ruengwaree, "Design of wide-band dipole antenna for digital TV broadcasting application," *2018 International Electrical Engineering Congress (iEECON)*, 1–4, IEEE, March 2018.

31. Wang, L., K. W. Chen, Q. Huang, W. H. Shao, W. X. Fang, G. G. Lu, and Y. F. En, "Wideband circularly polarized cross-dipole antenna with folded ground plane," *IET Microwaves, Antennas & Propagation*, Vol. 15, No. 5, 451–456, 2021.
32. Wen, L., S. Gao, B. Sanz-Izquierdo, C. Wang, W. Hu, X. Ren, and J. Wu, "Compact and wideband crossed dipole antenna using coupling stub for circular polarization," *IEEE Transactions on Antennas and Propagation*, 2021.
33. Li, D. Y., Y. C. Jiao, H. W. Yu, and Z. B. Weng, "Wideband circularly polarized pyramidal horn antenna based on spoof surface plasmon polaritons," *IEEE Transactions on Antennas and Propagation*, 2020.
34. Bayarsaikhan, P., R. Kuse, T. Fukusako, K. Tomimoto, M. Miyashita, and R. Yamaguchi, "Multi-port rectangular horn antenna with dielectric resonator for 5G application," *2021 IEEE Conference on Antenna Measurements & Applications (CAMA)*, 1–2, IEEE, November 2021.
35. Ishchenko, E. A., Y. G. Pasternak, V. A. Pendyurin, E. A. Rogozin, and S. M. Fedorov, "Horn antenna with integrated metamaterial for beam steering," *Journal of Physics: Conference Series*, Vol. 1902, No. 1, 012068, IOP Publishing, May 2021.
36. Fathi, E., F. Setoudeh, and M. B. Tavakoli, "Design and fabrication of a novel multilayer bandpass filter with high-order harmonics suppression using parallel coupled microstrip filter," *ETRI Journal*, 2022.
37. Manh, L. D., V. P. Hoang, and X. N. Tran, "A cost-effective 5-W GaN HEMT power amplifier for sub-6-GHz 5G wireless communications," *Mobile Networks and Applications*, 1–11, 2022.
38. Erkmen, F., T. S. Almoneef, and O. M. Ramahi, "Scalable electromagnetic energy harvesting using frequency-selective surfaces," *IEEE Transactions on Microwave Theory and Techniques*, Vol. 6, No. 5, 2433–2441, 2018.
39. Said, M. A. M., Z. Zakaria, M. N. Husain, M. H. Misran, and F. S. M. Noor, "2.45 GHz rectenna with high gain for RF energy harvesting," *Telkomnika*, Vol. 17, No. 1, 384–391, 2019.
40. Ard-Paru, N., *Managing Spectrum Commons in Thailand: Allocation and Assignment Challenges*, Chalmers University of Technology, 2012.